Spin excitations of individual magnetic dopants in an ionic thin film

To cite this article: Zhe Li *et al* 2022 *J. Phys.: Condens. Matter* **34** 475802

View the article online for updates and enhancements.

Spin excitations of individual magnetic dopants in an ionic thin film

Zhe Li[1,9,*] ⓘ**, Fernando Delgado**[2,9] ⓘ**, Mei Du**[1]**, Chen He**[1]**, Koen Schouteden**[3,4] ⓘ**,
Chris Van Haesendonck**[3] ⓘ**, Ewald Janssens**[3] ⓘ**, Andres Arnau**[5,6,7,*] ⓘ**, Peter Lievens**[3,*] ⓘ
and Jorge I Cerda[8]

[1] State Key Laboratory on Tunable Laser Technology, Ministry of Industry and Information Technology
Key Laboratory of Micro-Nano Optoelectronic Information System, School of Science, Harbin Institute
of Technology (Shenzhen), Shenzhen 518055, People's Republic of China
[2] Instituto de Estudios Avanzados IUDEA, Departamento de Física, Universidad de La Laguna, 38203
Tenerife, Spain
[3] Quantum Solid-State Physics, Department of Physics and Astronomy, KU Leuven, 3001 Leuven,
Belgium
[4] Semiconductor Physics Section, Department of Physics and Astronomy, KU Leuven, 3001 Leuven,
Belgium
[5] Departamento de Polímeros y Materiales Avanzados: Física, Química y Tecnología, Facultad de
Química, Universidad del País Vasco UPV/EHU, Apartado 1072, 20080 Donostia-San Sebastián, Spain
[6] Centro de Física de Materiales CFM/MPC (CSIC-UPV/EHU), Paseo Manuel de Lardizábal 5, 20018
Donostia-San Sebastián, Spain
[7] Donostia International Physics Center, Paseo Manuel de Lardizábal 4, 20018 Donostia-San Sebastián,
Spain
[8] Instituto de Ciencia de Materiales de Madrid, CSIC, Cantoblanco 28049 Madrid, Spain

E-mail: zhe.li@hit.edu.cn, andres.arnau@ehu.eus and peter.lievens@kuleuven.be

CrossMark

Abstract

Individual magnetic transition metal dopants in a solid host usually exhibit relatively
small spin excitation energies of a few meV. Using scanning tunneling microscopy and inelastic
electron tunneling spectroscopy (IETS) techniques, we have observed a high spin excitation
energy around 36 meV for an individual Co substitutional dopant in ultrathin NaCl films. In
contrast, the Cr dopant in the NaCl film shows much lower spin excitation energy around
2.5 meV. Electronic multiplet calculations combined with first-principles calculations confirm
the spin excitation induced IETS, and quantitatively reveal the out-of-plane magnetic
anisotropies for both Co and Cr. They also allow reproducing the experimentally observed
redshift in the spin excitations of Co dimers and ascribe it to a charge and geometry
redistribution.

[9] These authors contributed equally to this work.
[*] Authors to whom any correspondence should be addressed.

(Some figures may appear in colour only in the online journal)

Exploring the spin excitations of supported individual magnetic atoms is of great interest for fundamental understanding of magnetism towards the ultimate size limit [1], as well as for potential applications in data recording and information processing [2]. Significant progress has been achieved for single-atom magnets. This includes achieving the largest spin excitation energy of 58 meV among the 3*d* transition metal (TM) atoms for Co adatoms [1] or the long magnetic relaxation time and high magnetic stability for Ho adatoms below a temperature of 35 K and under fields up to 8 T [3–5], as well as the ability of reading, writing and manipulating the magnetic states of adatoms [2, 6–8]. However, these adatoms become mobile on surfaces above 50 K [4] and, hence, lose their single-atom-magnet properties. For practical applications at higher temperatures, designing thermally stable single-atom systems is required. Nowadays, it is well established that magnetic dopants in a solid host can have large binding energy and, thus, can be stable above room temperature [9, 10].

Concerning the observation of spin excitations in magnetic impurities on surfaces, a weak coupling between the magnetic atom and the underlying surface is required, as otherwise the hybridization between the magnetic atom and the surface states translates into broadening of the excitation peaks, even at low temperatures, and short spin relaxation time. This is the main reason why spin excitations have been investigated mainly in semiconducting [11], superconducting [12, 13] or insulating substrates [14] such as $Cu_2N/Cu(100)$ [15] and MgO/Ag(100) [1, 5] surfaces for 3*d* TM and 4*f* rare-earth atoms, both for adsorbed impurities and substitutional dopants. The case of substitutional dopants is more promising due their higher thermal stability. Another important requirement is a sizable magnetic anisotropy energy (MAE) that is higher than a few milli-electron volts, so that spin-flip excitations induced by the tunneling electrons appear as well-defined (sharp within the experimental energy resolution) peaks (or dips) in the measured derivative d^2I/dV^2 of the conductance dI/dV. Record MAE values have been observed for systems with large orbital moment and high spin–orbit coupling (SOC) [1]. These MAE values coincide with the so-called zero field splittings in the spin excitation spectrum. However, it is not clear whether a large MAE can also appear in systems with relatively reduced symmetry. For example, in a bulk fcc Co crystal the MAE is extremely low (almost negligible), being a fourth order effect in the SOC strength, but it becomes somewhat higher in bulk fct or hcp Co crystals [16], where it is of second order in the SOC strength with values of the order of 0.1 meV. Another extreme case of large magnetic anisotropy appears in low dimensional systems [17], where the MAE values can be as large as several meV. What remains to be

proven is whether another reduced symmetry case, like a crystal surface, permits sustaining large MAE values for 3*d* magnetic atom impurities.

In this work, we explore the case of a system like this, namely, bilayer NaCl/Au(111), that shows the same reduced crystal symmetry (square pyramidal) for Cr and Co substitutional dopants at Na sites [9, 10]. We show that the large MAE value observed for Co substitutional impurities is due to both a large orbital magnetic anisotropy, absent for Cr, and the different occupation of the *d*-shell ruled by strong electron correlation effects. We use scanning tunneling microscopy (STM) and inelastic electron tunneling spectroscopy (IETS) to measure the zero-field excitation (ZFE) energy of individual Co and Cr dopants embedded within an ionic thin NaCl film that is supported on the Au(111) surface. We demonstrate that single Co dopants show a very high spin excitation energy around 36 meV, the second largest spin-flip energy for a TM atom reported so far. In contrast, the embedded Cr atoms show a rather low spin excitation energy around 2.5 meV. Multiplet calculations accounting for the strong electron correlation indicate that there is a high spin excitation energy for Co while it is much lower for Cr, in good quantitative agreement with the measured ZFE.

Figure 1(a) presents an STM topography of three Co atomic dopants, where each of them replaces one Na ion (referred to as Co_{Na} hereafter) in the top surface of the NaCl film on Au(111) [9, 10]. One can observe an individual Co_{Na} dopant on the left, and on the right two Co_{Na} dopants forming a dimer with a Co–Co distance of 0.4 nm. Figure 1(c) shows a typical d^2I/dV^2 spectrum of the individual Co_{Na}. A spectrum of the surrounding NaCl surface (dashed black line in figure 1(c)) is added as a reference. The background-corrected d^2I/dV^2 by subtracting the d^2I/dV^2 on NaCl from the d^2I/dV^2 on Co is illustrated in figure 1(d). While the d^2I/dV^2 spectra show some variation across the NaCl surface (see figure S1 in supplementary information (SI) for more spectra), the d^2I/dV^2 spectra of the dopants always show a clear dip at negative voltage and a clear peak at positive voltage (figures 1(b)–(d)). We also extract the numerical derivatives of measured *I–V* curves, i.e. the corresponding dI/dV point spectra taken on top of individual Co_{Na} and on top the surrounding NaCl, as shown in figure 1(e). Figure 1(f) shows the background-corrected dI/dV on Co_{Na}, which exhibits a step-like increment in the conductance (dI/dV). Such spectroscopic feature of the Co_{Na} dopants is a typical signature of IETS, which can originate from a vibrational resonance or a spin excitation. The conductance change at the step in figure 1(e) is around 3 nS, which is a 38% increment with respect to the conductance (around 8 nS) of the step bottom. This large relative increment
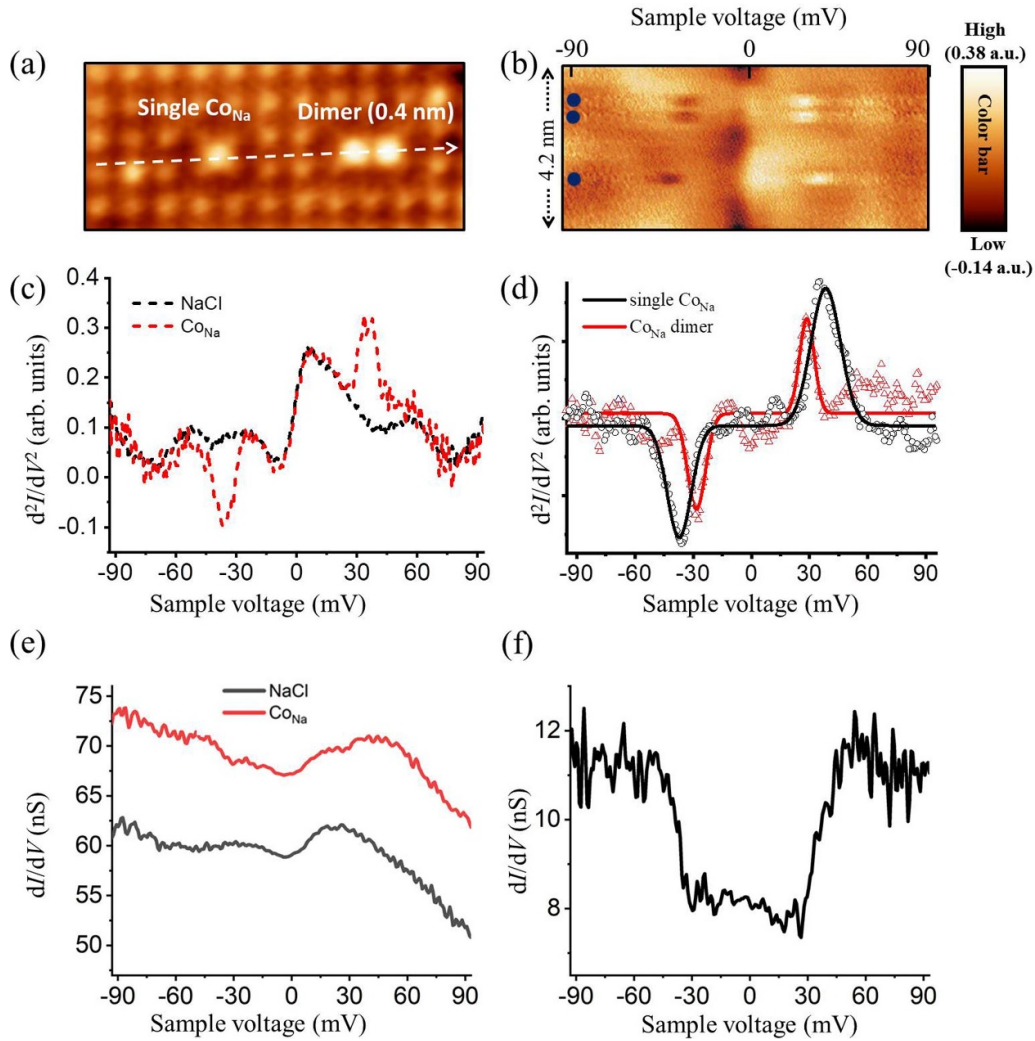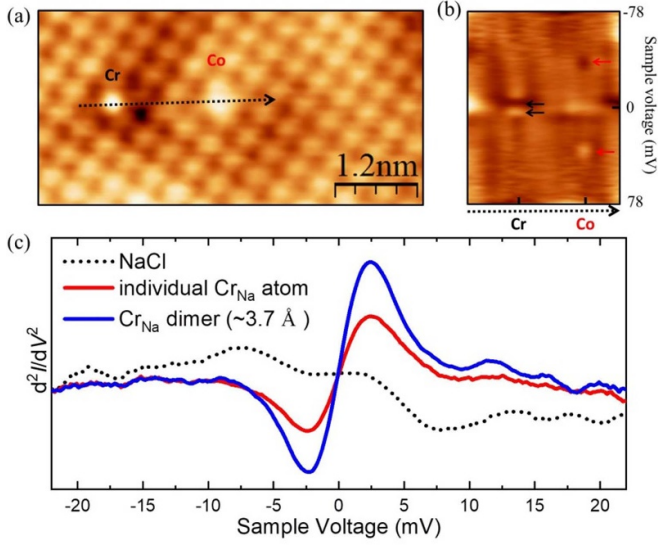
Figure 1. (a) The 5.0×2.3 N m^2 STM topography of an individual Co$_{Na}$ dopant and a Co$_{Na}$ dopant dimer. (b) Color visualization of $(d^2I/dV^2)(V)$ spectra taken along the white dashed line indicated in (a). The dark blue marks indicate the locations of the single dopant and the dimer. (c) d^2I/dV^2 spectra taken on a single Co$_{Na}$ dopant (dashed red curve) and on the surrounding NaCl surface (dashed black curve) in the immediate neighborhood of the Co dopant. (d) Background-corrected $(d^2I/dV^2)(V)$ spectra of the single Co$_{Na}$ dopant (black circles) and the Co$_{Na}$ dimer (red triangular). The solid lines are Gaussian fits. (e) Numerical dI/dV spectra on a single Co$_{Na}$ dopant (red curve) and on the surrounding NaCl surface (black curve) in the immediate neighborhood of the Co dopant. (f) Background-corrected (dI/dV) spectra of the single Co$_{Na}$ dopant. Setting point: $I = 1$ nA, $V = 50$ mV; lock-in modulation: 3 mV.

in conductance suggests that the IETS signal originates from the zero-field spin-flip excitation [18], while vibrational excitations typically result in a slight relative conductance increment with only a few percent [19, 20]. The Co$_{Na}$ dopants have zero-field spin-flip energy of around 36.2 meV, which is somewhat lower than that of Co adatoms on MgO [1] but still rather high. This is in line with the large excitation energies found for TM absorbed on top of highly electronegative elements such as O on MgO, with ZFEs of 58 meV for Co [1] and 15 meV for Fe [21], or N on a Cu$_2$N, with ZFE of 19 meV for Fe [22], but much larger than the values found for adatoms on lower symmetry films: 5–10 meV for Co on Cu$_2$N/Cu(001) [15] or 4 meV for Fe on Cu$_2$N/Cu(001) [23]. The ZFE found in the current work is remarkably large for single magnetic dopants, e.g. compared to values lower than 1 meV for the Fe dopants in InSb(110) [11], figures 1(b) and (d) also present the zero-field

spin-flip excitation of a Co$_{Na}$ dopant pair (Co–Co separation of 0.4 nm) with ZFE around 28.7 meV, showing a significant red shift of 20% with respect to the Co$_{Na}$ monomer.

Next, we compare the IETS behavior of Co$_{Na}$ dopants to that of Cr$_{Na}$ dopants. Figure 2(a) shows the STM topography image including a Co dopant and a Cr dopant. The two species can be distinguished by both the topographic appearance and the dI/dV resonances for the unoccupied local density of states as reported in previous work [9, 10]. Figure 2(b) presents a color visualization of d^2I/dV^2 spectra of the Cr$_{Na}$ and of Co$_{Na}$ shown in figure 2(a). Both spectra are measured with the same STM tip. As seen in figure 2(b), while the Co$_{Na}$ dopant exhibits a large IETS excitation energy around 36 meV, the Cr$_{Na}$ dopant only shows a rather small IETS excitation around 2.5 meV (see also red curve in figure 2(c)). Note that such a small excitation energy could be influenced by the effect of

Figure 2. (a) STM topography of a Cr_{Na} dopant and a Co_{Na} dopant. (b) Color visualization of $(d^2I/dV^2)(V)$ spectra taken along the black dashed arrow indicated in (a). The black arrows indicate the symmetric spin-flip excitations (±2.5 meV) for Cr_{Na}, while the red arrows indicate the spin excitations (±36 meV) for Co_{Na}. (c) d^2I/dV^2 spectra taken on a single Cr_{Na} dopant (red curve) and on a Cr_{Na} dimer (blue curve) using the same tip. Setting point: $I = 2$ nA, $V = 80$ mV; lock-in modulation: 2 mV.

temperature and/or bias modulation amplitude [24], which can be modeled as a convolution of the theoretical spectrum at vanishing temperature and modulation with a Gaussian of width: $W = \sqrt{(5.4k_BT)^2 + (1.72eU_{mod})^2}$. The observed resonance positions will not be shifted if the peak-dip distance ($2E_0$) is larger than the width W, while the peak will increasingly shift from the excitation energy and never appear below $0.42\,W$ if $2E_0$ becomes smaller than W [24]. In our case at 4.2 K and with modulation of 2 meV, the broadening W is about 4 meV, indicating that for excitation energies below 2 meV a shifted peak is expected. According to our simulation below, the excitation is around 2.5 meV, which may result in limited shift or some broadening in the measurements. We also notice that for the $S = 2$ Cr ions, the formation of a Kondo singlet will be strongly suppressed by the crystal anisotropy, which prevents the degeneracy of the lowest energy spin states [25, 26] and is supported by the absence of any zero-bias feature in our measurements. The significant difference between the IETS for Co and Cr is another observation that infers a magnetic and excludes a vibrational origin, since the vibrational modes for the Co and Cr systems are quite similar (see figure S2 in SI) and one thus would expect to observe similar vibrational excitations in IETS. The large difference (an order of magnitude) of spin excitation energy between Co and Cr cannot be explained by the difference in the SOCs ($\lambda_{Co}/\lambda_{Cr} \approx 3$) [27] alone. Another final observation is that for a Cr dimer, with interatomic separation around 0.4 nm, the spin excitation energy almost equals that of single Cr, as shown in figure 2(c), the difference being significantly smaller than the 4 mV broadening W.

Multiplet calculations are performed to calculate the spin excitations of the magnetic dopants, fully describing the correlations between the electrons on the $3d$-shell of the TM ion. In doing so, we only account for the e–e interaction between these electrons. The Coulomb matrix elements of this interaction can be calculated analytically by assuming a hydrogen-like wavefunction with an effective charge and radius [28]. This interaction can be easily parameterized in terms of a single parameter: the Hubbard U repulsion [29]. The effect of the surrounding ions is simulated by a point-charge model, i.e. each first and second neighbor atom is considered as a point charge without internal structure [28], with its magnitude and position extracted from a density functional theory (DFT) calculation, giving rise to the so-called *crystal field* (CF). Configuration mixing due to hopping to other TM orbitals or orbitals centered on different atoms (the '*ligand field*') is neglected. Although this point-charge model has strong quantitative limitations, it correctly reproduces the symmetries of the TM environment and it is particularly useful when combined with effective empirical values of the parameters at play [27]. Finally, the spin–orbit and Zeeman interaction with an external magnetic field are also included analytically [28].

For a free Co atom, the electronic configuration is $3d^74s^2$. According to Hund's rules, the ground state has spin and orbital angular momentum quantum numbers $S = 3/2$ and $L = 3$, respectively, corresponding to a ^4F electronic multiplet with multiplicity $(2S + 1)(2L + 1) = 28$ (neglecting the SOC). This is also the spin ground state of the energetically favorable Co substitutional ion in NaCl, as supported by our DFT calculations, which do not reveal a significant change in the occupation of the d-shell. When the Co atom is incorporated in the NaCl substrate, the electronic interaction with its environment breaks the rotational symmetry, partially lifting the $(2L + 1)$ orbital degeneracy. This is presented in figure 3(a). Contrary to the almost perfect axial symmetry found for TM atoms atop O on MgO [1, 21] or atop N on a Cu_2N surface [22], here the TM atom replaces a Na atom in the top-most atomic layer of the NaCl surface. Thus, it has five Cl ions as first neighbors and four Na ions as second neighbors. In the absence of lattice distortion, the resulting C_{4v} symmetry favors a degenerate d_{xz}, d_{yz} orbital ground state, with the Cl underneath pushing the d_{z^2} orbital higher in energy. This high orbital degeneracy is broken by a Jahn–Teller deformation. The atomic positions in the DFT calculations indicate a significant corrugation of the NaCl surface around the TM together with a mild, although sizable, rearrangement of electronic charge close to the magnetic dopant (see tables S1 and S2 in supplementary information). The total splitting of the ^4F multiplet induced by the CF is 0.44 eV. When switching on the SOC, the orbital motion of electrons changes with the orientation of the spin. Hence, the SOC partially splits the four-fold spin degeneracy, giving rise to Kramers' doublets. The effect of CF and SOC on the ground state energy level of Cr dopants is shown in figure S3(a) of the supplementary information. In brief, we find a spin ground state quintuplet ($S = 2$ and $L = 2$) with a low MAE = 2.5 meV. The main difference between the Cr and Co cases is the d-shell occupation. Due to d^4 occupation for Cr, the energy levels split in a completely different way from the
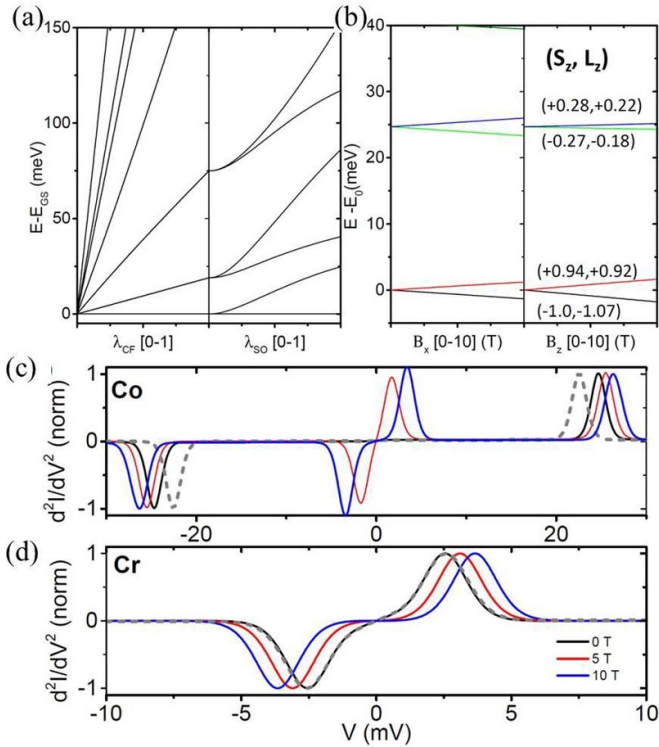
Figure 3. (a) Energy differences with respect to the ground state level versus the CF and spin–orbit strengths for Co dopants. (b) Low energy levels versus in-plane and out-of-plane fields for Co dopants. The labels indicate the expectation values of S_z and L_z at 5 T. (c) Simulated IETS of an individual Co dopant under various out-of-plane magnetic fields. (d) Simulated IETS of an individual Cr dopant under various out-of-plane magnetic fields. The dashed lines in (c) and (d) represent simulated IETS at 0 T of the Co and Cr dimers, respectively.

case of Co. The CF splits the ^5D state into five spin quintuplets, with the first excited quintuplet at approximately 250 meV above the ground state (see figure S3(a)). Then, the SOC fully breaks the spin degeneracy (figure S3(a)). The slightly broken symmetry of the surface induces a small quantum spin tunneling observed as a small splitting of the otherwise degenerate spin doublets.

The CF and the spin–orbit interaction link the orientation of the atom's orbital momentum with the spin. These interactions produce an energetically favorable direction for the magnetization M, i.e. a non-zero MAE. The magnetic field dependence of the energy spectrum is depicted in figure 3(b). When the magnetic field is applied along the out-of-plane z-axis, the ground state has $|S_z| \approx 1.0$, larger than the first excited state $|S_z| \approx 0.3$, indicating an out-of-plane easy axis. As observed, the presence of an unquenched orbital angular momentum gives place to an important mixing between the spin and orbital degrees of freedom. In addition, when $\boldsymbol{B}$ is along the x-axis, the magnetic-field induced splitting is smaller, as it corresponds to a hard axis. In the case of Cr, the CF gives rise to a finite quantum tunneling of magnetization (QTM), which leads to null expectation values of the angular momentum at zero field (see figure S4 in supplementary information). A high enough magnetic field can overcome the QTM and recover a finite

expectation value of the spin. The ground state at finite fields also corresponds to the maximum spin projection along the out-of-plane direction, indicating an out-of-plane easy axis. The MAE can be quantified by the energy difference between the ground state and the first excited state. Hence, the Co dopants have a calculated MAE of 25 meV atom^{-1}, as shown in figure 3(b). In contrast, the MAE for Cr dopants is only 2.5 meV. More details on the magnetic field dependence of Cr dopants are shown in figure S3(b).

In order to compare the experimentally measured dI/dV curves with theory, we combined the electronic multiplet calculations with a cotunneling theory where the TM d-orbitals are weakly hybridized with an STM tip and with the surface [30, 31], see calculation details in the supplementary information. Figures 3(c) and (d) show simulated IETS for Co and Cr, respectively, under various magnetic fields. In both cases, one observes a single inelastic spin transition with $|\Delta S_z| = 1$ [23], corresponding to a ZFE of the order of 25 meV atom^{-1} for Co, while the ZFE for Cr dopants is an order of magnitude lower. This indicates a low MAE for Cr, in very good agreement with the IETS data shown in figures 1 and 2. Notice that at finite out-of-plane magnetic field, the emergence of an additional low-energy spin excitation is expected for Co due to the mixing of the spin states introduced by the transversal crystal anisotropy.

Next, we discuss the multiplet calculations considering the charge distribution obtained for the Co dimers at a distance of 0.4 nm, extracted again from the DFT calculations. This is included in figure 3(c) as a dashed line. It reproduces very well the experimentally observed red shift of about 2.5 meV, with respect to the case of the Co monomer. Here, the charge of the neighboring atoms was considered as a free parameter. The simulations suggest that the red shift can be consistently associated to the charge redistribution induced by the second dopant. Conversely, simulations of anisotropic spin-models with isotropic ferromagnetic or antiferromagnetic exchange coupling (small compared with the local anisotropy) always displays a blue shift of the excitations, indicating that, in case of being present, this effect is of minor importance. This can be easily understood by taking into account that, due to the very large axial anisotropy, the interspin exchange takes the simple form of an Ising-type interaction. Since the excited doublet gains an approximated energy of $|J|/4$ and the ground state lowers its energy by $9|J|/4$ (neglecting the coupling between spin and orbital degrees of freedom), the excitation energy approximately increases by $\sim 10|J|/4$, independently of the sign of the coupling. Similar calculations do not show appreciable energy shifts for the Cr dimer, in good agreement with the experimental observations shown in figure 2.

In summary, we have combined STM/IETS experiments and multiplet calculations to explore and explain the magnetic anisotropy of two TM atoms, i.e. Co and Cr, that are substitutional dopants in bilayer NaCl films. We demonstrate that the Co dopants can maintain part of their large orbital moments with a large magnetic anisotropy in a reduced symmetry environment, translating into a high spin excitation energy around 36 meV under a dominant square pyramidal CF, while Cr atoms in the same environment show

a much lower spin excitation energy around 2.5 meV. Multiplet calculations, that include electron correlation effects, indicate that this difference is mainly due to the different occupation of the *d*-shell of these TM atoms that results in much stronger quenching of orbital angular momentum for Cr atoms. Hence, this study demonstrates that high magnetic anisotropy can be preserved in atomic dopant systems with high structural stability against elevated temperatures, which is crucial for room-temperature applications of single atom magnets.

Data availability statement

All data that support the findings of this study are included within the article (and any supplementary files).

Conflict of interest

The authors declare no conflict of interest.

ORCID iDs

Zhe Li https://orcid.org/0000-0002-6428-1222
Fernando Delgado https://orcid.org/0000-0003-2180-5273
Koen Schouteden https://orcid.org/0000-0002-5975-585X
Chris Van Haesendonck https://orcid.org/0000-0003-4944-1045
Ewald Janssens https://orcid.org/0000-0002-5945-1194
Andres Arnau https://orcid.org/0000-0001-5281-3212
Peter Lievens https://orcid.org/0000-0001-6570-0559

References

[1] Rau I G *et al* 2014 *Science* **344** 988
[2] Natterer F D, Yang K, Paul W, Willke P, Choi T, Greber T, Heinrich A J and Lutz C P 2017 *Nature* **543** 226
[3] Donati F *et al* 2016 *Science* **352** 318
[4] Natterer F D, Donati F, Patthey F and Brune H 2018 *Phys. Rev. Lett.* **121** 027201
[5] Donati F *et al* 2020 *Phys. Rev. Lett.* **124** 077204
[6] Yang K, Paul W, Phark S-H, Willke P, Bae Y, Choi T, Esat T, Ardavan A, Heinrich A J and Lutz C P 2019 *Science* **366** 509
[7] Yang K, Willke P, Bae Y, Ferrón A, Lado J L, Ardavan A, Fernández-Rossier J, Heinrich A J and Lutz C P 2018 *Nat. Nanotechnol.* **13** 1120
[8] Yang K, Phark S-H, Bae Y, Esat T, Willke P, Ardavan A, Heinrich A J and Lutz C P 2021 *Nat. Commun.* **12** 993
[9] Li Z *et al* 2014 *Phys. Rev. Lett.* **112** 026102
[10] Li Z, Chen H-Y T, Schouteden K, Janssens E, van Haesendonck C, Lievens P and Pacchioni G 2015 *Nanoscale* **7** 2366
[11] Khajetoorians A A, Chilian B, Wiebe J, Schuwalow S, Lechermann F and Wiesendanger R 2010 *Nature* **467** 1084
[12] Yazdani A, Jones B A, Lutz C P, Crommie M F and Eigler D M 1997 *Science* **275** 1767
[13] Heinrich B W, Pascual J I and Franke K J 2018 *Prog. Surf. Sci.* **93** 1
[14] Heinrich A J, Gupta J A, Lutz C P and Eigler D M 2004 *Science* **306** 466
[15] Oberg J C, Calvo M R, Delgado F, Moro-Lagares M, Serrate D, Jacob D, Fernandez-Rossier J and Hirjibehedin C F 2014 *Nat. Nanotechnol.* **9** 64
[16] Blanco-Rey M *et al* 2021 *ACS Appl. Nano Mater.* **4** 4398
[17] Gambardella P *et al* 2003 *Science* **300** 1130
[18] Loth S, Lutz C P and Heinrich A J 2010 *New J. Phys.* **12** 125021
[19] Komeda T 2005 *Prog. Surf. Sci.* **78** 41
[20] You S, Lü J-T, Guo J and Jiang Y 2017 *Adv. Phys.* X **2** 907
[21] Baumann S *et al* 2015 *Phys. Rev. Lett.* **115** 237202
[22] Rejali R, Coffey D, Gobeil J, González J W, Delgado F and Otte A F 2020 *npj Quantum Mater.* **5** 60
[23] Hirjibehedin C F, Lin C-Y, Otte A F, Ternes M, Lutz C P, Jones B A and Heinrich A J 2007 *Science* **317** 1199
[24] Balashov T, Miyamachi T, Schuh T, Märkl T, Bresch C and Wulfhekel W 2014 *Surf. Sci.* **630** 331
[25] Romeike C, Wegewijs M R, Hofstetter W and Schoeller H 2006 *Phys. Rev. Lett.* **97** 206601
[26] Romeike C, Wegewijs M R, Hofstetter W and Schoeller H 2011 *Phys. Rev. Lett.* **106** 019902
[27] Abragam A B B 1970 *Electron Paramagnetic Resonance of Transition Ions* (Oxford: Clarendon)
[28] Ferrón A, Delgado F and Fernández-Rossier J 2015 *New J. Phys.* **17** 033020
[29] Wolf C, Delgado F, Reina J and Lorente N 2020 *J. Phys. Chem.* A **124** 2318
[30] Reina Gálvez J, Wolf C, Delgado F and Lorente N 2019 *Phys. Rev.* B **100** 035411
[31] Delgado F and Fernández-Rossier J 2011 *Phys. Rev.* B **84** 045439